

Multi-Task Learning with Multi-Annotation Triplet Loss for Improved Object Detection

Meilun Zhou¹ 
University of Florida
Gainesville, FL, USA, 32611
zhou.m@ufl.edu

Aditya Dutt² 
University of Florida
Gainesville, FL, USA, 32611
aditya.dutt@ufl.edu

Alina Zare¹ 
University of Florida
Gainesville, FL, USA, 32611
azare@ufl.edu

¹Department of Electrical and Computer Engineering ²Department of Computer and Information Science and Engineering

Abstract—Triplet loss traditionally relies only on class labels and does not use all available information in multi-task scenarios where multiple types of annotations are available. This paper introduces a Multi-Annotation Triplet Loss (MATL) framework that extends triplet loss by incorporating additional annotations, such as bounding box information, alongside class labels in the loss formulation. By using these complementary annotations, MATL improves multi-task learning for tasks requiring both classification and localization. Experiments on an aerial wildlife imagery dataset demonstrate that MATL outperforms conventional triplet loss in both classification and localization. These findings highlight the benefit of using all available annotations for triplet loss in multi-task learning frameworks.

Index Terms—Deep learning, multi-task learning, triplet loss, object detection, classification

I. INTRODUCTION

Multi-task learning is a learning paradigm where a single model is trained to simultaneously perform multiple tasks by using complementary task information from different task representations. Previously, multi-task learning frameworks have shown promise for optimizing classification and localization objectives [1]. However, many existing loss functions like cross-entropy or mean squared error may lack the capacity to capture the nuanced interdependencies between these objectives [2]. Triplet loss, a popular metric learning approach, excels at class separation in latent spaces and is highly effective for tasks requiring robust classification [3]. However, the emphasis and sole requirement of class similarity often limits the applicability of triplet loss in scenarios requiring precise localization. Triplet loss effectively separates classes but does not inherently incorporate any information derived from box annotations needed for accurate localization.

Recently, aerial imagery has emerged as a powerful tool for observing animals across vast and remote areas [4]. Wildlife detection is crucial for ecosystem management, biodiversity conservation, and environmental policy-making. Object detection algorithms that automatically detect objects are essential for analyzing large amounts of image data. This application provides a real-world problem for investigating adding different types of annotations to triplet loss because this task inherently involves two objectives: classifying detected objects into different categories and localizing them within images using bounding boxes. The complexity of natural habitats

combined with variability in animal appearances and challenging conditions like occlusion or diverse lighting increases the difficulty of wildlife detection [5]. Traditional loss functions, including cross-entropy and mean squared error, often fail to capture the nuanced interdependencies between classification and localization tasks [2].

This study introduces a Multi-Annotation Triplet Loss (MATL) designed to address these limitations. By integrating bounding box annotations alongside class labels, the proposed method constructs a latent space that balances both the demands of classification and localization. The addition of bounding box annotations specifically provides information about various features of the boxes, like size or symmetry. Evaluation of MATL on wildlife detection in aerial imagery highlights the approach’s ability to enhance the shared representation space for multi-task learning by effectively leveraging information from all available label sources.

II. PROPOSED METHODOLOGY

Traditional triplet loss approaches effectively group similar samples while separating dissimilar ones based solely on class labels. However, class labels may be insufficient for more complex tasks requiring both identification and localization. We propose a modified triplet loss function that incorporates the bounding box annotation information alongside class labels to create a latent space designed for the multi-task objectives of object classification and precise localization. The following subsections review the standard triplet loss formulation, detail our method of integrating bounding box annotations into our modified triplet loss, and outline the network architecture designed for wildlife detection in aerial imagery.

A. Triplet Loss Formulation

The standard triplet loss is commonly used in metric learning to differentiate between embeddings of similar and dissimilar samples [3]. The loss operates on a set of three samples: an anchor sample a , a positive sample p , and a negative sample n . For each anchor sample, the positives and negatives are determined using the class labels y . Anchor and positive belong to the same class, while the negative belongs to a different class than the anchor. The triplet loss objective is to ensure that the distance between the anchor and positive

embeddings is smaller than the distance between the anchor and negative embeddings by at least a margin α . In this manner, triplet networks cluster different classes in the latent space by focusing on class information.

The loss function is formulated as follows:

$$\mathcal{L}_{triplet}(a, p, n, y) = \max(d(f(a), f(p)) - d(f(a), f(n)) + \alpha, 0), \quad (1)$$

where f is the embedding function or feature extractor, α is the margin (set by the user) enforced between positive and negative samples, and d is a distance function.

B. Multi-Annotation Triplet Loss Formulation

We include bounding box characteristics as an additional annotation within the triplet loss framework to improve the model’s ability to learn multi-task representations. While standard triplet loss uses only class labels to guide embedding separation, our approach integrates bounding box information by defining new discrete box labels based on the spatial characteristics of the target object’s box annotations. Specifically, this study focuses on the addition of two key bounding box properties: box size and symmetric squareness.

The box area feature was calculated by multiplying the width and height of each target object’s bounding box, providing a direct measure of the object’s spatial extent. Symmetric squareness was determined by calculating the minimum of the width-to-height ratio and the height-to-width ratio, subtracted from 1. A ratio closer to 0 indicates a more symmetric or square-like box shape. This feature distinguishes between objects of different areas and symmetry to provide an additional dimension for separating the box features.

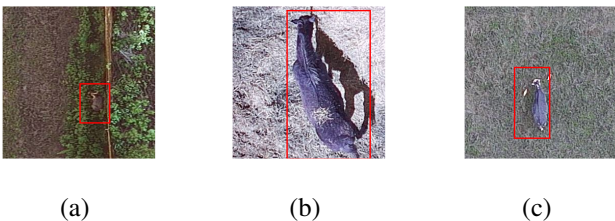


Fig. 1: Examples of three different box classes present in aerial imagery. (a) Deer, a small-square box, (b) Horse, large-elongated box, (c) Cow, small-elongated box.

We then applied K-means clustering [6] on the box area, symmetric squareness, width, and height values to categorize bounding box information. By clustering these features into three distinct groups, three new “labels” that correspond to varying box size and squareness profiles were created. The new box labels, along with their corresponding RGB image, are shown in Fig. 1. The number of clusters was chosen using the Elbow Method [7] where the within-cluster sum of squares displayed a distinct inflection point. These clusters capture common bounding box patterns across objects, enabling the model to generalize better to objects with similar spatial characteristics while maintaining distinctions in class.

Prior to clustering, all features were independently normalized using Min-Max normalization to ensure uniform scaling and eliminate magnitude discrepancies across dimensions using the formula:

$$x' = \frac{x - \min(x)}{\max(x) - \min(x)}, \quad (2)$$

where $\min(x)$ and $\max(x)$ represent the minimum and maximum values of the feature x across the dataset, respectively. This normalization step guarantees that all features contribute equally to the clustering objective, preventing dominance by features with larger ranges.

With the new box labels assigned to each sample, we first implemented a triplet loss focused on the box labels based off Equation 1:

$$\mathcal{L}_{box} = L_{triplet}(a, p, n, y_{box}), \quad (3)$$

where y_{box} are the three different types of box labels. Then, the typical class label triplet loss is formulated as:

$$\mathcal{L}_{class} = L_{triplet}(a, p, n, y_{class}), \quad (4)$$

where y_{class} are the class labels. Our proposed loss, Multi-Annotation Triplet Loss (MATL), combines the traditional class-based triplet loss with an additional triplet loss component that operates on these box labels. These two triplet losses shape the latent space simultaneously. The complete loss function is expressed as:

$$\mathcal{L}_{MATL} = (1 - \lambda) \mathcal{L}_{class} + \lambda \mathcal{L}_{box}, \quad (5)$$

where the hyperparameter λ controls the weight of the box label triplet loss relative to the class label loss. This hyperparameter allows for fine-tuning of the contribution from each label type. Setting λ closer to 1 emphasizes box label information, while lower values prioritize class differentiation. In this paper, we distinguish raw box annotations, the dataset’s ground truth boxes, from user-generated box labels derived through K-means clustering.

C. Network Architecture

The network architecture in this study consists of an auto-encoder design aimed at extracting feature representations for two downstream tasks: classification and binary mask segmentation. The encoder extracts multi-scale features from images using dilated convolutions, starting with 16 filters and increasing to 512. The decoder reconstructs the binary mask by upsampling the encoded vector with transposed convolutions and residual connections. The final convolutional layers with sigmoid activation produce a mask, where pixel values over 0.5 represent the target region. During inference, a bounding box is then fitted around the largest connected component. The classifier head is a fully connected network with four hidden layers. Batch normalization and ReLU activations stabilize training after each layer. The final layer uses softmax activation to output probabilities for three target classes.

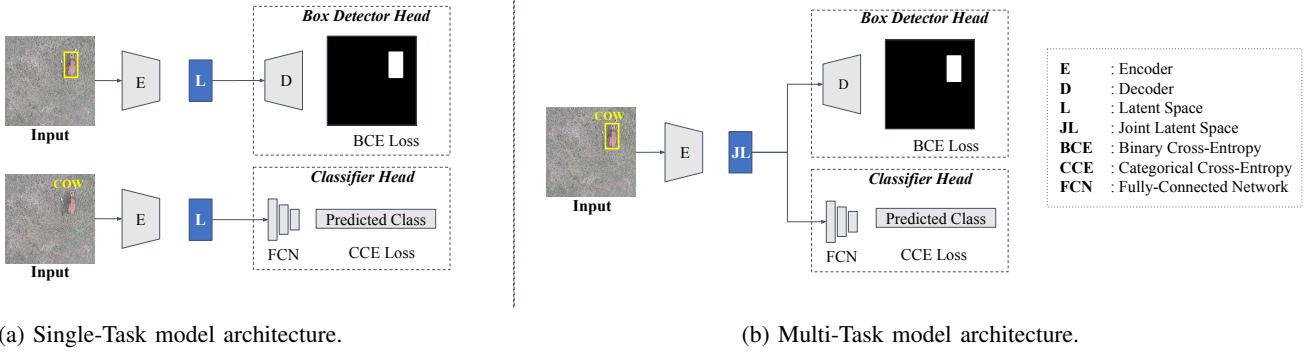


Fig. 2: (a) Single-Task and (b) Multi-Task model architectures.

In the multi-task setup, the embeddings produced by the encoder serve as a shared representation for multiple task-specific heads in parallel. Each task-specific head processes these joint embeddings independently to predict outcomes for its respective task. This design allows the encoder to learn features that generalize across all tasks in order to leverage complementary information from multiple objectives. In contrast, the single-task setup restricts the encoder embeddings to flow into a single task-specific head, which focuses the feature extraction entirely on the needs of the individual task. While single-task setups may optimize performance for the single task, the restriction may limit the encoder’s ability to learn features that capture broader, cross-task relationships. The setups are displayed in Fig. 2.

All models were trained with Tensorflow on an NVIDIA A100 GPU with 12 CPUs and 60 GB of memory allocated. This configuration provided the computational resources necessary for efficient training and optimization. Code can be found at <https://github.com/GatorSense/MATL/tree/main>.

III. EXPERIMENTAL RESULTS

The Animal Wildlife Image Repository (AWIR) [8] is a dataset created to support research in wildlife detection, classification, and monitoring. AWIR contains a collection of RGB images capturing various species of animals in their natural environments. We first cropped images containing animals into smaller tiles of size 300×300 pixels. Each tile includes only a single animal, which simplifies the model’s task by focusing attention on a single target per image. To avoid bias in the object’s location within each tile, we employed a random cropping strategy around the animal that ensures that the animal is not always centered. Therefore, the model learns to detect the object regardless of position in the image. All images were normalized using the same MinMax normalization in Equation 2 before passing into the network. The box annotations were clustered and the mean values of the area and symmetric squareness features from each cluster are further detailed in Table I.

We compared the multi-task model’s performance to the models without the triplet loss and with the standard class-label-based triplet loss, while keeping all model architectures

TABLE I: The mean normalized area and symmetric squareness (SS) values used in bounding box portion of the Multi-Annotation Triplet Loss.

Category	Norm. Area	Norm. SS
Small-Elongated Box	0.088	0.621
Large-Elongated Box	0.630	0.559
Small-Square Box	0.093	0.173

identical. The classification and box localization tasks are evaluated using the overall classification accuracy and Intersection over Union (IoU), respectively. All models were trained and validated eight different times with 30% of the total data using a stratified K-fold technique where $K = 8$. These models were then tested on the remaining 70% of the data. Average results of the experiments are shown in Table II.

We empirically determined the best weight λ for MATL for this dataset to be 0.25 after testing values of 0.25, 0.5, and 0.75. For the classification task, the MATL consistently outperforms both models without triplet loss and the class-label triplet loss in single and multi-task setups. For the box detection task, the MATL at 0.25 weight performs comparably to without triplet loss and demonstrates clear improvement over the class-label triplet loss. An example of this improvement in localization is shown in Fig. 3.

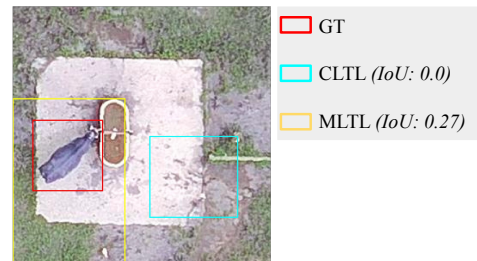


Fig. 3: An example of the improved box localization from MATL as compared to CLTL for class cow.

TABLE II: Results of Single-Task (ST) and Multi-Task (MT) models on classification and box localization tasks are presented. Multi-Annotation Triplet Loss (MATL) is compared with Without Triplet Loss (WTL) and Class Label Triplet Loss (CLTL) across both models and tasks. MATL results with box triplet loss weights (λ) of 0.25, 0.5, and 0.75 are reported. For classification, mean overall accuracy (%) and standard deviation across eight experiments are reported; for box localization, mean IoU and standard deviation are provided.

Model	Classification (Accuracy)					Box Localization (Intersection over Union)				
	WTL	CLTL	MATL (0.25)	MATL (0.5)	MATL (0.75)	WTL	CLTL	MATL (0.25)	MATL (0.5)	MATL (0.75)
Single-Task	58.2 ± 6.1	73.3 ± 1.5	83.0 ± 2.3	79.4 ± 2.6	79.9 ± 4.3	0.190 ± 0.025	0.157 ± 0.022	0.184 ± 0.017	0.185 ± 0.018	0.185 ± 0.015
Multi-Task	67.8 ± 3.9	78.1 ± 5.0	83.2 ± 1.7	81.9 ± 2.6	80.1 ± 3.0	0.178 ± 0.013	0.149 ± 0.025	0.189 ± 0.016	0.177 ± 0.018	0.179 ± 0.012

IV. DISCUSSION

The new latent space supervised by both class and box labels proves beneficial for multi-task, since both the classification and box tasks are improved, whereas the classification label embedding space shows a classification task dominance. By using both class label and box annotation supervision, the MATL is able to better leverage information from both tasks and outperform the models without triplet loss and class label triplet loss. The effect of the weight λ for the box annotations on the overall MATL is important to consider since classification performance decreases as λ increases. The result is an improvement over traditional single-task methods [9] and class-label triplet loss, which tend to focus on one task at the expense of the other.

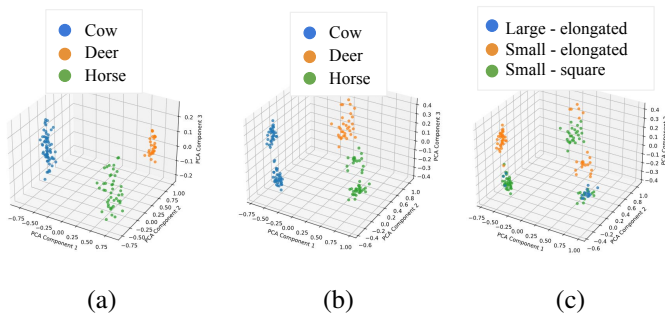


Fig. 4: A comparison between different representations after applying Principal Component Analysis (PCA) is shown. (a) Class-label embeddings colored by class labels, (b) Multi-Annotation embeddings colored by class labels, and (c) Multi-Annotation embeddings colored by box labels.

Fig. 4 (a) provides a comparative visualization of the latent space representations learned under different configurations of the triplet loss. In Fig. 4 (a), where the triplet loss is based solely on class labels, the embeddings form distinct clusters, with each cluster corresponding to a specific class. This demonstrates that the learned representation effectively captures inter-class separability. However, this approach assumes uniformity among samples within each class, neglecting any inherent intra-class variations that may be essential for certain tasks like object localization. In contrast, Fig. 4 (b) illustrates the latent space when both class and bounding box labels are

incorporated into the triplet loss. The embeddings are colored by the class labels to show the variations within each class. The resulting latent space exhibits sub-clusters within each class cluster, reflecting variations among samples of the same class. These sub-clusters capture meaningful differences, such as variations in bounding box dimensions (*e.g.*, width and height), which are critical for accurate localization. This suggests that samples within the same class are not always identical in their spatial properties, and these differences are naturally embedded in the latent representation. A similar pattern can be observed in Fig. 4 (c) when the embeddings are colored by box labels: “large-elongated box”, “small-elongated box,” and “small square box.” The “small-elongated box” class forms multiple clusters within all class clusters because this type of box is present in all three animal classes. Similarly, “small-square box” is present mostly in deer and cow classes. The horse class consists mostly of “large-elongated box” which is indicated by the less scattered single cluster.

To summarize, by leveraging multiple attributes for each sample, the model captures a more comprehensive representation of the data. This approach maps similar samples closer together based on several characteristics, rather than relying on a single label. The resulting latent space is more robust and improves performance across tasks by considering the diverse aspects of each sample.

V. CONCLUSION

The proposed Multi-Annotation Triplet Loss improves multi-task scenarios by encouraging a more structured and meaningful representation of the data. This approach enhances the model’s ability to handle multiple tasks simultaneously by encouraging the model to learn features that are shared across different types of labels. One direction moving forward is to explore a multi-modality approach [10], incorporating thermal data alongside other data types. Thermal data can provide complementary information, especially in low-light conditions, so combining thermal imagery with high-resolution RGB imagery could improve the model’s robustness and accuracy [11]. Additionally, instead of forcing both labels to share a single latent space, future work will investigate methods of combining information from two different labels, such as using concatenation or other effective fusion strategies. This would allow for more flexible and task-specific representations.

REFERENCES

- [1] Y. Wang, W. Ding, R. Zhang, and H. Li, "Boundary-aware multitask learning for remote sensing imagery," *IEEE Journal of selected topics in applied earth observations and remote sensing*, vol. 14, pp. 951–963, 2020.
- [2] A. Hermans, L. Beyer, and B. Leibe, "In defense of the triplet loss for person re-identification," *arXiv preprint arXiv:1703.07737*, 2017.
- [3] E. Hoffer and N. Ailon, "Deep metric learning using triplet network," in *Similarity-based pattern recognition: third international workshop, SIMBAD 2015, Copenhagen, Denmark, October 12-14, 2015. Proceedings 3*. Springer, 2015, pp. 84–92.
- [4] J. A. Elmore, M. F. Curran, K. O. Evans, S. Samiappan, M. Zhou, M. B. Pfeiffer, B. F. Blackwell, and R. B. Iglay, "Evidence on the effectiveness of small unmanned aircraft systems (suas) as a survey tool for north american terrestrial, vertebrate animals: a systematic map protocol," *Environmental Evidence*, vol. 10, no. 1, p. 15, 2021.
- [5] M. Zhou, J. A. Elmore, S. Samiappan, K. O. Evans, M. B. Pfeiffer, B. F. Blackwell, and R. B. Iglay, "Improving animal monitoring using small unmanned aircraft systems (suas) and deep learning networks," *Sensors*, vol. 21, no. 17, p. 5697, 2021.
- [6] A. Likas, N. Vlassis, and J. J. Verbeek, "The global k-means clustering algorithm," *Pattern recognition*, vol. 36, no. 2, pp. 451–461, 2003.
- [7] P. Bholowalia and A. Kumar, "Ebk-means: A clustering technique based on elbow method and k-means in wsn," *International Journal of Computer Applications*, vol. 105, no. 9, 2014.
- [8] S. Samiappan, B. S. Krishnan, D. Dehart, L. R. Jones, J. A. Elmore, K. O. Evans, and R. B. Iglay, "Aerial wildlife image repository for animal monitoring with drones in the age of artificial intelligence," *Database*, vol. 2024, p. baae070, 2024.
- [9] A. Lakkapragada, E. Sleiman, S. Surabhi, and D. P. Wall, "Mitigating negative transfer in multi-task learning with exponential moving average loss weighting strategies (student abstract)," in *Proceedings of the AAAI Conference on Artificial Intelligence*, vol. 37, no. 13, 2023, pp. 16 246–16 247.
- [10] A. Dutt, A. Zare, and P. Gader, "Shared manifold learning using a triplet network for multiple sensor translation and fusion with missing data," *IEEE Journal of Selected Topics in Applied Earth Observations and Remote Sensing*, vol. 15, pp. 9439–9456, 2022.
- [11] B. S. Krishnan, L. R. Jones, J. A. Elmore, S. Samiappan, K. O. Evans, M. B. Pfeiffer, B. F. Blackwell, and R. B. Iglay, "Fusion of visible and thermal images improves automated detection and classification of animals for drone surveys," *Scientific Reports*, vol. 13, no. 1, p. 10385, 2023.